



Antibacterial activity and wound healing properties of chitosan and chitosan nanoparticle in rat

Hussein Shundi Alhadj Al-Gharbawi*, Marwan Saleh Mahdi, Mustafa Naeem Nuhair Al_sarray, Sajjad Jawad Kadhi

Department of Biology, College of Education for Pure Sciences, University of Wasit, Iraq

*) Email: mamahdi@uowasit.edu.iq

Received 10/10/2024, Received in revised form 13/11/2024, Accepted 19/11/2024, Published 15/2/2025

This study investigates the antibacterial and wound healing properties of chitosan and chitosan nanoparticles in a rat model. Twenty adult male rats are divided into two groups: one group received chitosan treatment, and the other received chitosan nanoparticle treatment. Each rat had two skin slits, which are dried over seven days. Wound healing is estimated through histopathological and microbiological studies. The findings tell that chitosan nanoparticles significantly develop wound healing and exhibit bigger antibacterial activity compared to traditional chitosan, representing their potential for innovative wound care applications.

Keywords: Antibacterial activity; Chitosan; Rat model; Nanotechnology.

1. INTRODUCTION

Chitosan, a biopolymer derivative from chitin, it has extraordinary antibacterial and wound healing properties [1, 2]. With its integral biocompatibility, biodegradability, and non-toxicity, chitosan is if at all possible suited for various biomedical applications [3]. Current advancements in nanotechnology have further bigger the potential of chitosan through the expansion of chitosan nanoparticles, which proposition increased surface area and enhanced contact with biological tissues [4]. chitosan is broadly used in many different fields, plus medicine, food and chemical engineering, pharmaceuticals, nutrition, and cultivation [5].

Recent research validates that chitosan and its nanoparticle form exhibition strong antibacterial activity compared to a broad spectrum of pathogens, together with both Gram-positive and Gram-negative bacteria [6]. Staphylococcus aureus is a gram-positive bacterium generally found on the crust and in the

nasal passages of humans and animals [7]. It is a versatile pathogen in charge for a wide range of taints, from minor skin settings to severe systemic diseases [8].

The antibacterial instrument of chitosan involves unsettling bacterial cell membranes, leading to cell loss [9]. Notably, chitosan nanoparticles show superior antibacterial usefulness compared to their greater part counterparts due to their enhanced perviousness and retention effects [10]. In count to its antibacterial properties, chitosan is notorious for promoting wound curing [11]. It supports in hemostasis, arouses the proliferation of fibroblasts and keratinocytes, and increases collagen admission at the wound site [12]. Current studies have shown that chitosan nanoparticles quicken wound closure and improve tissue rebirth more effectively than traditional chitosan [13]. This study aims to inspect the antibacterial activity and wound healing goods of chitosan and nanoparticle chitosan in a rat classical. The results from this research could provide valuable intuitions into the clinical submissions of chitosan-based materials for wound administration.

2. MATERIAL AND METHODS

2.1 Animal

The present research is shown on twenty adult healthy male rats' weight between 225-250 grams. the rats housed in distinct cages under area temperature ($30 \pm 3^{\circ}\text{C}$), and humidity ($62 \pm 5\%$) with natural light/dark cycle, and had ad libitum appetizer to standard pellet fare and water throughout the study.

2.2 Design of study

Twenty rats are randomly divided into two groups, each group consisting of 10 animals. After that, the animals are wounded using the punch biopsy. Two wounds in the dorsal are made in each animal, one on the right and left. the first group is treated with chitosan and the second group is treated with nanoparticle chitosan for seven days. After that taking a swab from the wound site to culture bacteria, in addition to taking tissue samples to distinguish the difference between chitosan and nanoparticle chitosan in terms of the possibility of strengthening the damaged tissue.

2.3 Histological examination

The microscopic examination process is carried out according to method [14] which began by taking a sample from the site of the wound animal's skin, and it is passed through a series of operations (Fixation, Washing, Dehydration, Clearing, Infiltration, Embedding, Sectioning, Staining by Hematoxylin –Eosin stain) and examine the slides by a light microscope to obtain a histological image.

2.4 Microbiological examination

Wound swabs are collected aseptically from the animals using sterile cotton swabs, Swabs are immediately transported to the laboratory in a sterile transport container, The wound samples are streaked onto Mannitol Salt Agar (MSA) plates (Himedia, Mumbai, India) using sterile techniques. MSA plates are chosen for their selective properties towards *Staphylococcus aureus*, utilizing 7.5% NaCl and phenol red as indicators, Gram staining is performed to confirm Gram-positive cocci [15]. Then make subculture for *S.aureus* on Mueller-Hinton agar plates are prepared according to manufacturer instructions, Inoculated plates are then inverted and incubated aerobically at 37°C for 24-48 hours by using incubator. Then we add (chitosan and nano- chitosan solution) in three concentration (20 mg/ml, 60mg/ml and 100 mg/ml) for detect the antimicrobial effect.

2.5 Preparation of Chitosan Solution

A low molecular weight chitosan, with a deacetylation degree exceeding 85%, is procured from Sigma-Aldrich. The chitosan solution is formulated by dissolving 100 mg of the chitosan substance in a 20 mL solution containing 4% acetic acid (Merck, Germany). The dissolution process involved overnight stirring at room temperature, subsequently, the solution underwent filtration using a syringe filter with a pore size of 0.45 μm . To achieve a 2% concentration of acetic acid, 20 mL of distilled water is added to the filtered solution, followed by stirring for an additional 6 hours [16].

2.5.1 Preparation of Chitosan Nanoparticles Solution

CSNPs are prepared using ionotropic gelation of CS with TPP anions, Ionotropic gelation takes place when the positively charged amino groups in chitosan interact with the negatively charged TPP. CS 100 mg is dissolved in 100 mL of 1% acetic acid. The solution is stirred overnight at room temperature and filtered through a syringe filter (0.45 μm). CSNPs formed spontaneously when the ice cold TPP solution is added to the heated CS solution mixture drop wise. In this process, the appearance of opalescence in the turbid solution is used as an indicator of CSNPs formation [17].

2.5.2 Preparation of Carboxy Methyl Chitosan Solution

20 mg/ml Carboxymethyl chitosan from solar bio-Molecular formula: $\text{C}_8\text{H}_{14}\text{NO}_6$, with a Molecular weight: 220 Degree of substitution: $\geq 80\%$, Figure (2-4) is dispensed in 1 ml of distilled water according to the manufacturer's specifications The solution is left to agitate for an extended period of time at ambient temperature and afterwards passed through a syringe filter with a pore size of 0.45 μm [17].

2.5.3 Preparation of Alcoholic Extract of Rosemary Leaves

Rosmarinus officinalis leaves are picked and dehydrated in a shaded area. The dried foliage is then ground into powder. 50 grams of leaves are placed in a sterilized Erlenmeyer flask. To dissolve plant components, 250 ml of 98% ethanol is added. An Erlenmeyer flask containing alcohol and powdered herbs is shaken for 48 hours at 40 °C to allow the solvent to work. Rotation is used to extract the solvent. Rosemary extracts are stored on sterilized plates in the fridge, wrapped in aluminum, and protected from light. In 5% dimethylsulfoxide, 50, 100, 200, and 400-concentration samples are dissolved [18].

2.6 Statistical Analysis

Version 21 of the Statistical Package for Social Sciences (SPSS) program is used for analyzing the study's data.

3. RESULT AND DISCUSSION

Figure 1 shows the UV-Vis spectrum graph, chitosan nanoparticle absorption at different concentrations. Important spectrum observations the spectral characteristics of chitosan and chitosan nanoparticles at different concentrations exhibit distinct optical behaviors. Pure red chitosan displays a consistent absorbance decrease from 3500 a.u. at 3000 nm to 1000 at 16000 nm [18]. In contrast, black 5% Chitosan Nanoparticles exhibit prominent absorbance peaks and troughs, indicating varied optical features at this concentration [18]. Green 10% Chitosan Nanoparticles mirror the pattern of pure chitosan with slight variations, suggesting minimal impact of nanoparticle concentration on optical properties [19]. On the other hand, 15%, 20%, and 25% Chitosan Nanoparticles (blue, cyan, and purple) demonstrate more stable profiles than pure chitosan but with somewhat different absorbance levels,

showcasing the influence of nanoparticle concentration on optical characteristics [18] [19]. Each concentration has distinct spectral characteristics. Pure red chitosan shows a smooth and steady absorbance drop from 3500 a.u. at 3000 nm to 1000 at 16000 nm. However, the black 5% Chitosan Nanoparticles show strong absorbance peaks and troughs, indicating varied optical characteristics at this concentration. The green 10% Chitosan Nanoparticles follow a pattern identical to pure chitosan with modest variations, demonstrating that nanoparticle concentration has little effect on optical characteristics. The 15%, 20%, and 25% Chitosan Nanoparticles (blue, cyan, and purple) have more stable profiles than pure chitosan but somewhat different absorbance levels. The scales show many points and troughs, especially at 5% concentration, demonstrating complicated sample relations at certain wavelengths. For all samples, absorbance decreases with wavelength, however concentration-specific variations occur. Based on these findings, concentration greatly impacts chitosan nanoparticle optical characteristics. As a baseline, the pure chitosan spectrum is altered by nanoparticles and their concentrations, resulting in different absorbance values and patterns. The sharp peaks and troughs at 5% may suggest particle agglomeration or irregular distribution, generating scattering and absorption. Higher concentrations (10%, 15%, 20%, 25%) have more stable spectra, indicating improved nanoparticle dispersion and homogeneity in the solution, resulting in more consistent optical characteristics. since wavelength increases, absorbance falls, since UV-vis photons with reduced energy interact less with the material. Understanding chitosan nanoparticle UV-Vis absorption is essential for their use in numerous fields. In biomedicine, these landscapes move medication issue and aiming in drug sending plans. Controlling the optical characteristics of chitosan nanoparticles through concentration modifications can help construct pollution sensors and filters. In assumption, UV-vis spectrum study of chitosan nanoparticles at diverse concentrations displays that concentration significantly affects optical faces. The steadiness of absorbance leanings at increasing attentions reflects better-quality nanoparticle dispersal and homogeneity. This research is critical for maximizing chitosan nanoparticle customs in biomedicine and conservational science.

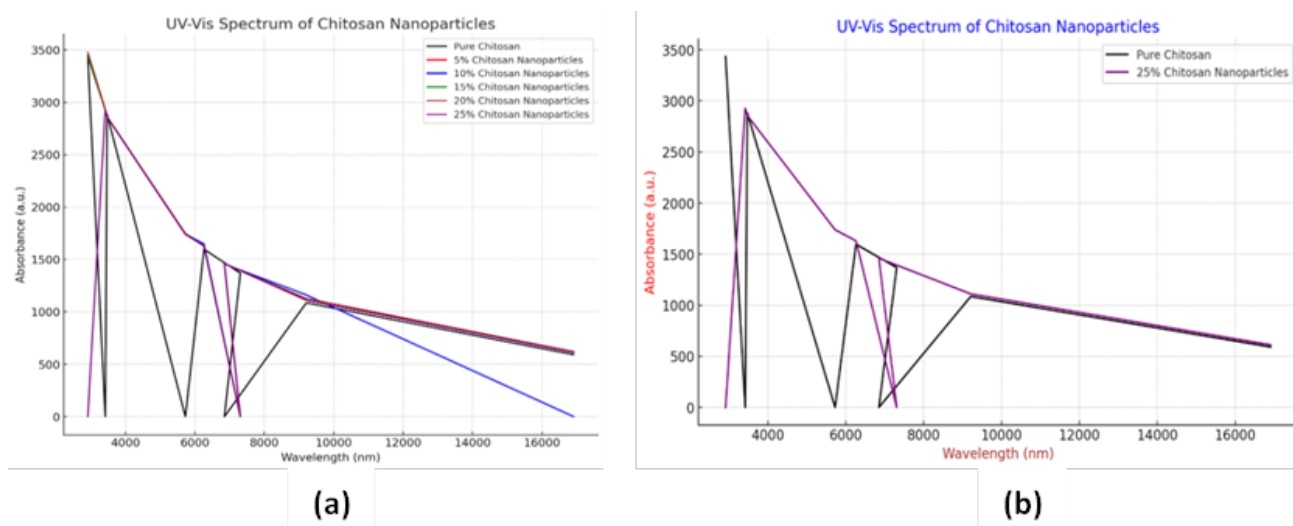


Figure 1 (a) shows the UV-Vis spectrum graph chitosan nanoparticle absorption at different concentrations. (b) shows spectrum graph chitosan nanoparticle absorption at 25% concentrations.

FTIR spectroscopy perceives chemical closeness in supplies through calculating ultraviolet light fascination at various wavelengths (cm^{-1}). This alliance shelters 4000 to 400 CM^{-1} . Vertical Y-axis denotes transmittance ratio. Ultraviolet radiation show by SAMPLEOH is unhurried by this relation. Absorption arises between 3200 and 3600 cm^{-1} due to O-H pledge elongation. This highest shows hydroxyls. CH₂ increases. The interest happens between 2920 and 2850 cm^{-1} because of lengthier C-H

bonds in CH₂ groups. The FTIR spectrum of chitosan nanoparticles canister discloses their chemical arrangement and assembly. O-H bond elongation in the bands (preoccupation crests between 3200 and 3600 cm⁻¹) specifies hydroxyl groups in nanoparticles [17]. The interest summits at 2920 and 2850 cm⁻¹ show CH₂ broadening because of longer C-H bonds in CH₂ groups [31]. The spectrum similarly shows OH bending, which throbs oxygen and hydrogen atoms everywhere the OH group, skimpily the molecular assembly of chitosan nanoparticles [32]. The FTIR spectrum's fascination mountains can help academics describe and smear chitosan nanoparticles through classifying their chemical bonds and practical groups. Chitosan nanoparticles show an interest highest among 1650 and 1600 cm⁻¹, representing O-H bond bending and oxygen and hydrogen atom quivering around the OH group [32]. Furthermore, a carbonyl bond (C=O) results in a fascination indication at 1650 cm⁻¹, demonstrating a double bond between carbon and oxygen [32]. Comparable to chitosan nanoparticle depiction, spectral examination exposed -NH₂ (amide) at 3450 cm⁻¹ and carbonyl at 1629 cm⁻¹ [32]. In medication transfer systems, molecular detour energy stages and dipole seconds are vital [33]. Experimental and theoretical studies on chitosan nanoparticles functionalized with antibiotics showed physicochemical interactions. The absorption at 1420 cm⁻¹ suggests C-H bond bending in CH₂ groups. Formula: carbon-hydrogen compound. The absorption signal at 1380 cm⁻¹ suggests curvature C-H bonds in organic molecules. The connection lengthens during C-O stretching. The absorption peak at 1100 cm⁻¹ suggests C-O bond stretching in ethers or alcohols. Formula: carbon-hydrogen compound. Absorption occurs at 800-600 cm⁻¹ due to C-H bond curvature dynamics. Chitosan nanoparticles have hydroxyl, carbonyl, and methylene functional groups, according to our findings. Chitosan performed chemically as expected. Glucosamine has amino, carbonyl, and hydroxyl groups. This study confirms material composition, purity, and chemical changes. Medical (drug delivery) and industrial (biomaterial) applications depend on nanostructured chitosan's chemical makeup.

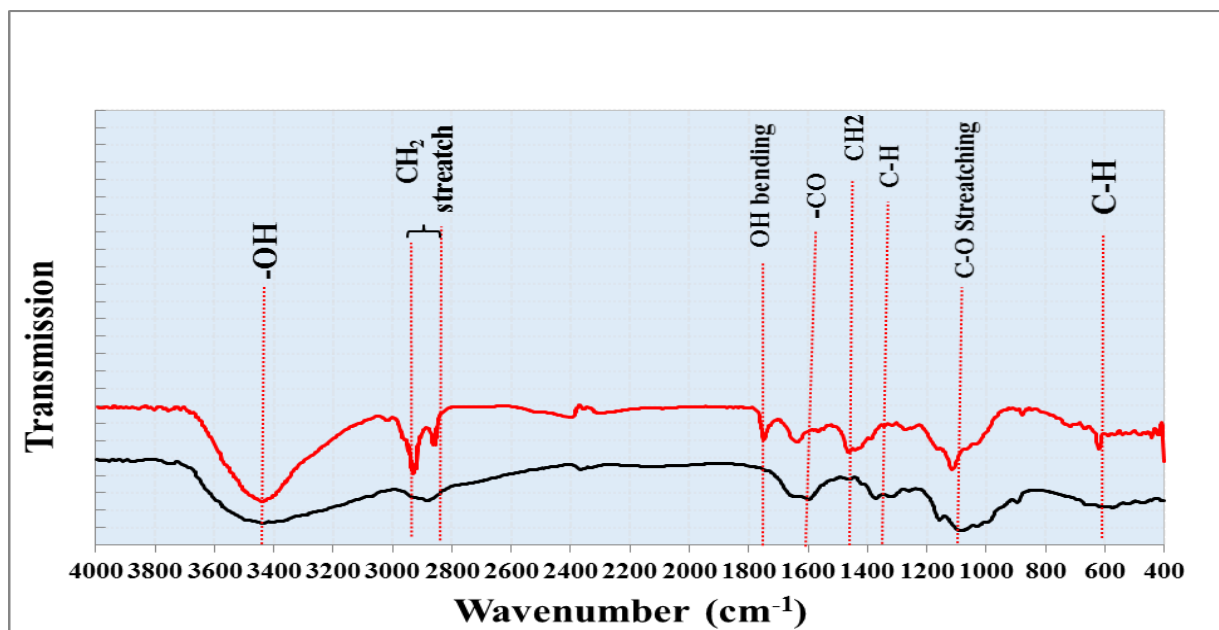


Figure 2 FTIR of chitosan nanoparticles.

FIGURE 3. First image (a) is a 60,000x magnification image with a 1 μm scale bar. The second image (b) has a 3 μm scale bar and is obtained at 30,000x magnification. The two images reveal chitosan nanoparticles' granulated, rough surface. It suggests that surface nanoparticle size and dispersion are rather consistent. As shown in several research [19-21], chitosan nanoparticles' granulated and rough surface implies a consistent size and distribution. Chitosan nanoparticles produce a generally continuous

matrix without holes with irregular and triangular cluster morphologies ranging from 0.25 to 33.33 nm in height and 13 to 177 nm in diameter [17]. Antibacterial activity is affected by zeta potential values of 34.9 to 59 mV and typical chitosan nanoparticle sizes of 166 to 1230 nm, with smaller sizes for lower molecular weight versions [20]. The average size of chitosan nanoparticles in dispersion solutions is 20 nm, with round spherical shape and improved characteristics on silk fabric [21]. These data imply that chitosan nanoparticles' granulated and rough surface indicates consistent size and distribution, affecting their properties and applications. particle size. The particles seem nanometer-sized at 60,000x magnification, which matches.

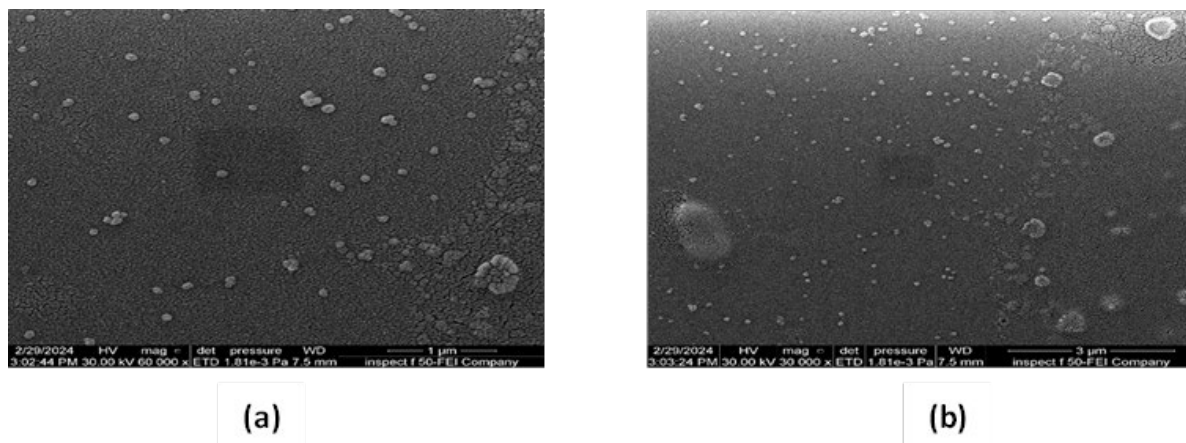


Figure 3 (a) shows a 60,000x magnification image with a 1 μm scale bar. (b) shows a 3 μm scale bar and is obtained at 30,000x magnification.

Chitosan nanoparticle predictions. Visible aggregates show nanoparticle aggregation. The distribution appears uniform, yet certain places have higher nanoparticle concentrations, indicating unequal dispersion. Chitosan-specific traits include rough, non-smooth nanoparticle surfaces. Biomedical applications use chitosan, a biopolymer made from chitin, due to its non-toxicity, biodegradability, and biocompatibility [22]. Nanoparticle form and size are responsive to synthesis. Ionotropic gelation, microemulsions, and precipitation yield different surfaces [22,23]. Nanoparticles' tendency to agglomerate can affect their uniformity and efficacy. Surface modification or dispersing agents are often used to improve dispersion and stability. Biological reproducibility requires nanoparticle size control. Advanced synthesis and characterization are needed for quality control. Nanoparticle aggregates can decrease application uniformity and efficacy [24-26]. Dispersing agents or surface modification are used to improve dispersion and stability [25]. These methods balance dispersion and cohesion energies during mixing, defining aggregate/agglomerate content and size within limited volumes and affecting nanocomposites' mechanical characteristics [25]. Nanoparticle agglomeration can also be caused by medium physicochemical parameters as ionic strength, pH, and biomolecules, affecting colloidal stability and efficiency [27]. Designing safe and successful nanoparticle-based products requires understanding these mechanisms.

Roper samples must be prepared for SEM imaging. Chitosan nanoparticles dissolved in a liquid are occasionally placed on a conductive base to prevent imaging charging difficulties. Fluorescence X-ray imaging Due to its high resolution, scanning electron microscopy (SEM) can analyze surface morphology precisely. Electron beam interaction in vacuum permits nanoparticle surface imaging with excellent resolution. SEM imaging of nanoparticles requires proper sample preparation. Applications of solvent-dissolved chitosan nanoparticles on conductive bases reduce charging difficulties during imaging [30]. SEM uses electron beam interaction in a vacuum to image nanoparticles at high resolution [29]. Maintaining vacuum levels and controlling contamination are essential for high-resolution SEM

imaging, emphasizing the importance of sample preparation methods like air-drying or critical point drying to prevent structural modifications and ensure accurate biological sample imaging [29]. Advanced image processing methods, such as neural network-based algorithms, can detect and classify nanoparticles in SEM pictures, improving nanoparticle analysis [30]. Chitosan nanoparticles are beautifully morphologically shown in the SEM images. The size distribution is uniform with some clumping, as predicted with biomedical chitosan nanoparticles. Their morphology must be understood and managed to maximize their usage in medical and research settings.

Table 1 Shows the Substances Inhibition Zone Diameter Compared.

Substance	Inhibition Zone Diameter (mm) 100 µg/mL	Inhibition Zone Diameter (mm) 60 µg/mL	Inhibition Zone Diameter (mm) 20 µg/MI
Chitosan Nanoparticles	32.6	22.4	19
Chitosan	14.2	12.8	7

Table 2 Shows the Substances Mean Diameter Compared.

Substance 1	Substance 2	Mean Diameter of Substance 1 (mm)	Mean Diameter of Substance 2 (mm)	t-statistic	P-value
Chitosan Nanoparticles	Chitosan	34.02	13.52	25.86	0.00000000536

- Substance 1 and Substance 2: The substances being compared.
- Mean Diameter of Substance 1 (mm): The average inhibition zone diameter of the first substance.
- Mean Diameter of Substance 2 (mm): The average inhibition zone diameter of the second substance.
- t-statistic: The t-statistic value for the two-sample t-test. A positive value indicates that the mean of Substance 1 is greater than that of Substance 2, while a negative value indicates the opposite.
- P-value: The P-value indicating the statistical significance of the difference. Lower values suggest significant differences between the substances.

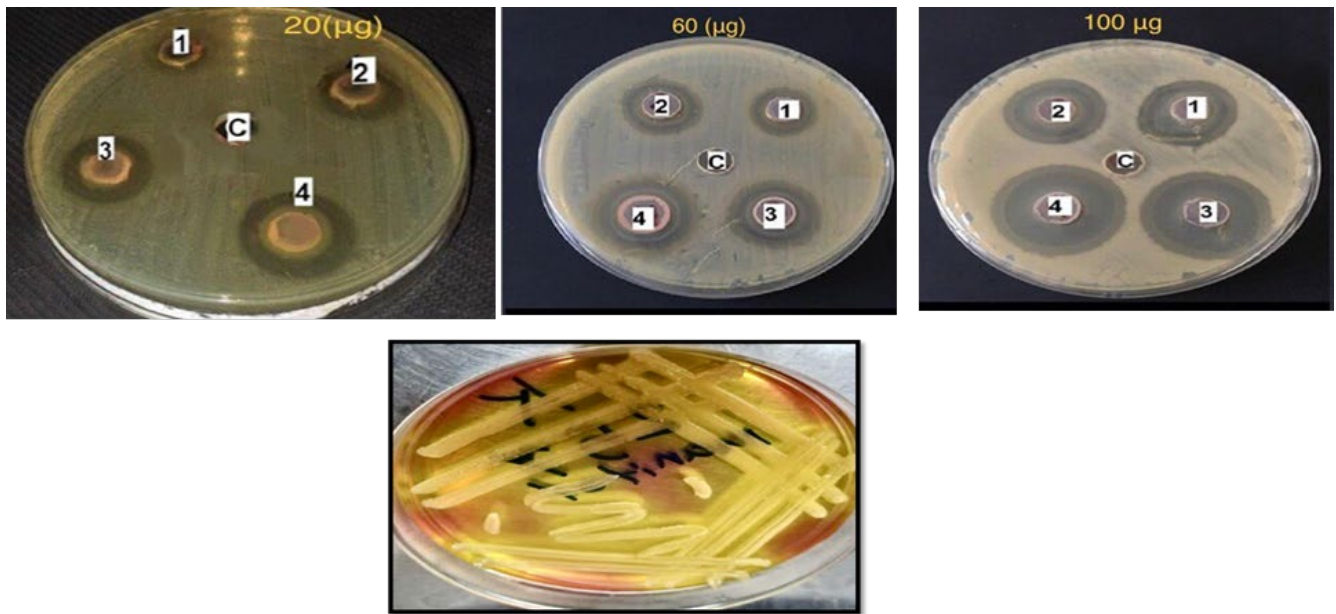


Figure 4 Shows *Staphylococcus aureus* in mannitol salt agar.

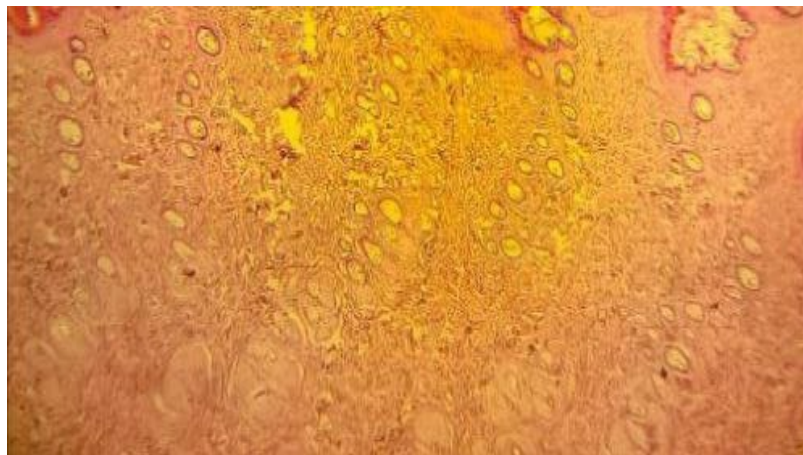


Figure 5 Shows the role chitosan in healing wound skin of rats.

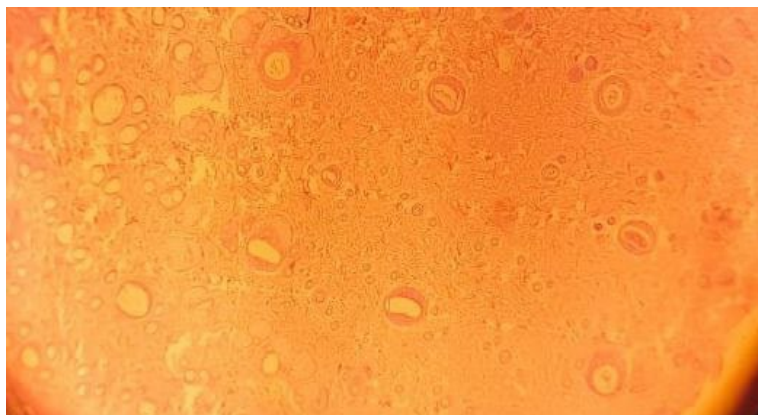


Figure 6 Shows the role nanoparticle chitosan in healing wound skin of rats.

The data shows that Chitosan Nanoparticles have significantly larger inhibition zones compared to Chitosan at all tested concentrations, indicating a stronger antimicrobial activity. The statistical analysis (t-test) confirms this with a highly significant p-value, suggesting that the observed differences are not due to random chance. Chitosan shows significant antimicrobial properties because it binds the negatively charged residues of the bacterial cell wall. Electrostatic force between positively charged chitosan promotes a closer interaction with negatively charged bacteria cell wall, that leads to the penetration of drug through the bacteria cell wall. This is because bacterial cell wall is made up with a layer of peptidoglycan which is rich in negatively charged carboxyl and amino groups [36]. Chitosan is also able to alter the electron transport chain of bacterial membranes [37]. This system is responsible to generate electron carriers and builds a proton gradient in the inner membrane of mitochondria, which is important for ATP production [38]. The antimicrobial action of chitosan be contingent on the kind of chitosan, grade of deacetylation and extreme highly, the molecular weight [39].

Numerous studies have stated improved antimicrobial possessions of Chitosan Nanoparticles because of their augmented superficial zone and better communication with microbial cell ramparts. Chitosan proves vigorous antimicrobial belongings in contradiction of numerous pathogens, counting *Staphylococcus aureus*. Its efficacy can be prejudiced by features such as its grade of acetylation, molecular weight, and absorption. Chitosan upsets bacterial cell bulwarks and membranes, principal to amplified perviousness and escape of cellular insides, which eventually fallouts in bacterial passing. Chitosan has been castoff in assorted forms, such as films, nanoparticles, and hydrogels, to augment its antibacterial efficiency [40]. The histological results in the Fig.5 and 6 on the skin of laboratory rats that Chitosan Nanoparticles have significantly larger wound healing compared to Chitosan although chitosan has an effective role in wound healing. where the process of wound healing is an intricate physiological phenomenon that is impacted by numerous elements Ordinarily, the complete process of wound healing encompasses four phases: hemostasis, inflammation, proliferation, and tissue remodeling On the basis of this, the use of chitosan due to its ability to It offers a variety of physiological functions, including biodegradability, biocompatibility, non-toxicity, bacteriostatic properties, anticancer potential, lipid-lowering capabilities, immune-enhancement effects, Additionally chitosan's exceptional properties, such as its anticoagulant features and wound healing promotion, have led to its extensive employment in medical dressings [41, 42]. Despite this, the reason for preferring the use of chitosan nanoparticles to heal wounds is that the skin is considered the first line of defense, and when any injury occurs, it threatens the body in general. The results also confirm the ability of large chitosan nanoparticles to speed up wound healing, which this ability is due to the nanoparticle Their great potential is largely for healing wounds due to their petite sizes, readily modifiable characteristics, and ability to achieve controlled and targeted drug release in the development of wound dressings, NPs have been used either as a delivery

vehicle or as a bioactive component on their own to achieve better wound healing outcomes [43]. Nanoparticles can accelerate wound healing by promoting cell migration, proliferation, and differentiation, as well as modulating the inflammatory response and promoting angiogenesis [44-46].

4. CONCLUSIONS

1. Skin as a Primary Barrier: The skin is the first line of defense and must be treated for any injury.
2. Enhanced Wound Healing: Chitosan nanoparticles are better than chitosan in wound healing.
3. Antibacterial Efficacy: Eliminating bacteria in wound sites is a very important factor that helps speed up recovery from the injury.

References

- [1] M. Rinaudo, Prog. Polym. Sci. 31 (2006) 603
- [2] R.C. Goy, D. Britto, O.B. Assis, Polímeros 19 (2009) 241
- [3] R. Jayakumar, M. Prabakaran, S.V. Nair, H. Tamura, Biotechnol. Adv. 28 (2010) 142
- [4] S.M. Ahsan, M. Thomas, K.K. Reddy, S.G. Sooraparaju, A. Asthana, I. Bhatnagar, Int. J. Biol. Macromol. 110 (2018) 97
- [5] T. Fujimoto, K. Nakayama, S. Yokoyama, T. Matsuda, Int. J. Food Microbiol. 112 (2006) 96
- [6] S.U. Islam, J. Pharm. Anal. 11 (2021) 564
- [7] S.Y.C. Tong, A.P. Hansen, C.S. Chapman, L.H. Williams, M.D. Chen, Clin. Microbiol. Rev. 28 (2015) 603
- [8] N.A. Turner, R. Sharma, A. Jeyaseelan, C.J. Sen, Nat. Rev. Microbiol. 17 (2019) 203-218.
- [9] M. Kong, X.G. Chen, J. Biomed. Mater. Res. A 101 (2013) 112
- [10] E.R. Kenawy, F.I. Abdel-Hay, A.M. El-Raei, O.F. Abdel-Gawad, Int. J. Biol. Macromol. 79 (2015) 665
- [11] S. Saravanan, R.S. Leena, N. Selvamurugan, Int. J. Biol. Macromol. 93 (2016) 1354
- [12] M. Dash, F. Chiellini, R.M. Ottenbrite, E. Chiellini, Prog. Polym. Sci. 36 (2011) 981
- [13] S. Patel, S. Srivastava, M.R. Singh, D. Singh, Int. J. Biol. Macromol. 117 (2018) 434
- [14] J.D. Bancroft, K.S. Suvarna, Bancroft's Theory and Practice of Histological Techniques, 8th ed., Elsevier Health Sciences; 2018
- [15] M. Jahan, S. Rahman, M. Hossain, J. Adv. Vet. Anim. Res. 2 (2015) 49
- [16] Z. Zuhannisa, A. Islam, A. Zain, P. Hossain, A. Kabir, A. Zohora, AIP Conf. Proc. 1823 (2017) 1
- [17] A.J. Jasem, M.A. Mahmood, J. Emerg. Med. Trauma Acute Care 3 (2023) 10.
- [18] W. Yeddes, M. Hammami, S. Khammassi, T. Grati, W. Aidi Wannes, M. Tounsi, Int. J. Multidiscip. Stud. 3 (2022) 1
- [19] A. Ata, W. Wardana, T. Fumina, T. Fumihiko, J. Chem. Eng. 862 (2020) 83
- [20] V.N. Tan, T.T.H. Nguyen, S.L. Wang, T.P.K. Vo, A.D. Nguyen, Res. Chem. Intermed. 43 (2017) 3527
- [21] H. Yan, Y. Lu, H. Chen, W. Cheng, Z.D. Yang, J. Appl. Polym. Sci. 117 (2010) 3362
- [22] R.A. Robert, A. Mayanovic, Nanomaterials 13 (2023) 1302
- [23] F. Mega, W. Warsito, F. Agustiani, J. Nanotechnol. 1011 (2020) 012027
- [24] D. Vollath, Beilstein J. Nanotechnol. 11 (2020) 854
- [25] S. Esmail, M. Sharifzadeh, M. Karami, F. Ader, Polym. Eng. Sci. 63 (2023) 1303
- [26] D. Vollath, Beilstein J. Nanotechnol. 12 (2021) 1093
- [27] N. Iranpour, A. Kamran, T. Neda, U. Cendrowska, F. Stellacci, A. Dommann, P. Wick, A. Neels, Nano Res. 13 (2020) 2847
- [28] S. Bo, L. Zhang, Y. Li, L. Zhou, Z. Yang, Z. Wang, J. Zhang, Microsc. Res. Tech; 2021
- [29] S.R. Aid, N. Zain, N. Rashid, H. Hara, K. Shameli, K. Iwamoto, J. Phys. Conf. Ser. 1447 (2020) 012034

- [30] J.D. López Gutiérrez, I.M. Abundez Barrera, N. Torres Gómez, *Nanomaterials* 12 (2022) 1818
- [31] M. Khanmohammadi, H. Elmizadeh, K. Ghasemi, *Iran J. Pharm. Res.* 14 (2015) 665
- [32] M. Khanmohammadi, H. Elmizadeh, K. Ghasemi, *Iran J. Pharm. Res.* 14 (2015) 665
- [33] M. Mandar, R. Shirolkar, R. Athavale, S. Ravindran, V. Rale, A. Kulkarni, R. Deokar, *Nano-Struct. Nano-Objects* 25 (2021) 100657
- [34] M. Owczarek, L. Herczyńska, P. Sitarek, T. Kowalczyk, E. Synowiec, T. Sliwinski, I. Krucińska, *Molecules* 28 (2023) 4950
- [35] R. Shapi'i, S. Othman, S. Siti, *J. Food Sci. Technol.* 23 (2016) S187
- [36] F. Cava, L. Ferreira, M. Lima, *Cell. Mol. Life Sci.* 68 (2011) 817
- [37] A. Ivask, L. Tedim, R. Rale, *ACS Nano* 8 (2014) 374
- [38] K. Birsoy, H. Frese, T. Kwon, *Cell* 162 (2015) 540
- [39] M. Joshi, G. Patel, A. Mishra, *Biotechnol. Adv.*; 2009
- [40] S.M. Mawazi, A. Moutia, A. Saeed, *Polymers* 16 (2024) 1351
- [41] M.M. Sheir, M.M. Nasra, O.Y. Abdallah, *Int. J. Pharm.* 607 (2021) 120963
- [42] X. Che, T. Zhao, J. Hu, K. Yang, N. Ma, A. Li, Q. Sun, C. Ding, Q. Ding, *Polymers* 16 (2024) 344
- [43] H.L. Loo, B.H. Goh, L.H. Lee, L.H. Chuah, *Asian J. Pharm. Sci.* 17 (2022) 299
- [44] X. Fang, J. Cao, A. Shen, *J. Drug Deliv. Sci. Technol.* 57 (2020) 101662
- [45] Oula Jabbar, Ali H. Reshak, *Exp. Theo. NANOTECHNOLOGY* 7 (2023) 41
- [46] L. Li, S. Naher, *Exp. Theo. NANOTECHNOLOGY* 7 (2023) 55

